Journal of Power Sources 193 (2009) 441–446

Contents lists available at ScienceDirect

Journal of Power Sources

journal homepage: www.elsevier.com/locate/jpowsour

Enhancement of electrocatalytic activity of platinum for hydrogen oxidation reaction by sonochemically synthesized WC_{1-x} nanoparticles

Juyeong Kim[a], Ji-Hoon Jang[b], Yang-Hee Lee[b], Young-Uk Kwon[a,b,*]

[a] SKKU Advanced Institute of Nanotechnology, Sungkyunkwan University, Suwon 440-746, Republic of Korea
[b] Department of Chemistry, BK-21 School of Chemical Materials Science, Sungkyunkwan University, Suwon 440-746, Republic of Korea

ARTICLE INFO

Article history:
Received 21 January 2009
Received in revised form 9 March 2009
Accepted 25 March 2009
Available online 11 April 2009

Keywords:
Tungsten carbide
Platinum
Nanoparticle
Sonochemistry
Hydrogen oxidation reaction
Fuel cell

ABSTRACT

Two types of composite materials composed of Pt and WC_{1-x} nanoparticles supported on multiwalled carbon nanotubes (MWNT) are synthesized and evaluated in terms of their electrochemical properties, especially for the hydrogen oxidation reaction (HOR). The Pt nanoparticles are prepared by reduction of H_2PtCl_6 with $NaBH_4$, and the WC_{1-x} nanoparticles by a sonochemical method with a $W(CO)_6$ precursor. One of the composites is synthesized by forming WC_{1-x} nanoparticles on Pt-loaded MWNT and the other by physically mixing Pt-loaded MWNT with WC_{1-x}-loaded MWNT. The sonochemical synthesis of WC_{1-x} on Pt-loaded MWNT forms WC_{1-x} preferentially on Pt nanoparticles, which makes intimate contact between WC_{1-x} and Pt nanoparticles. The cyclic voltammograms of these composite materials show evidences for H^+-spill-over from Pt to WC_{1-x}, thereby increasing the electrochemically active surface area (ECA). The composite in which WC_{1-x} is deposited on Pt shows a remarkable increase in ECA probably because the intimate contact between WC_{1-x} and Pt enhances the H^+-spill-over. These materials exhibit enhanced HOR characteristics with Pt-specific mass activities about twice that of pure Pt nanoparticles.

1. Introduction

Fuel cells are promising energy providers, but their widespread commercialization requires some important issues to be resolved. The development of inexpensive electrocatalysts with high activity is key objective. At present, Pt/C, in the anode and cathode of polymer electrolyte fuel cells, and PtRu/C, in the anode of direct methanol fuel cells, are known to be the most active materials [1]. Nevertheless, the high cost and the CO poisoning of Pt poses serious problems and has therefore prompted many researchers to seek new electrocatalyst materials that can completely or partly replace Pt.

Tungsten carbides have long been considered to be a substitute for Pt because their band structures are reported to be similar to that of Pt [2–4]. Indeed, an early study in the 1970s demonstrated a fuel cell with tungsten carbide used as the hydrogen oxidation reaction (HOR) catalyst although the activity was orders of magnitudes lower than that of Pt [5]. Later, Nagai et al. [6] observed that an anode electrocatalyst composed of tungsten carbide alone generated a power density that was 5.7% of that of with Pt. Recently, there have been many attempts on using tungsten carbide to enhance the catalytic activity for the HOR [7,8] and the methanol oxidation reaction [9–11], and to increase the CO tolerance in electrocatalysis at anodes [12–15]. Furthermore, when a small amount of platinum was added to tungsten carbide, the catalytic activity was reported to increase dramatically [7–10]. In addition, it has been found that the onset potential of oxygen reduction reaction can be increased by incorporating tungsten carbide in the cathode [16,17]. Some reports mentioned that the electrochemically active surface area (ECA) of platinum supported on WC or W_2C increased by 2–3 times compared with that on carbon supports [9,10,14,18]. The behaviour was explained by H^+-spill-over between platinum and tungsten carbide.

There are three phases of tungsten carbide, namely W_2C, WC (or α-WC), and WC_{1-x} (or β-WC). While the first two are thermodynamic phases, the last is a high-temperature phase that is stable above 2785 °C [19]. The conventional method to synthesize tungsten carbides is the carburization of tungsten oxide powder or ammonium metatungstate at high temperatures (~1000 °C) [20]. Therefore, the phases obtained from such methods are restricted to WC and W_2C. It has been shown that the electrocatalytic activity for the HOR increases in the order of $WC > WC_{1-x} > W_2C$ [7]. Probably with this background information, the current emphasis is on the WC phase. There have been a few investigations of W_2C as an electrocatalyst, but it has been found to be unstable [21]. With the lack of a proper synthetic method for high surface

* Corresponding author at: Department of Chemistry, BK-21 School of Chemical Materials Science, Sungkyunkwan University, Suwon 440-746, Republic of Korea. Tel.: +82 31 290 7070; fax: +82 31 290 7075.
E-mail address: ywkwon@skku.edu (Y.-U. Kwon).

0378-7753/$ – see front matter © 2009 Elsevier B.V. All rights reserved.
doi:10.1016/j.jpowsour.2009.03.070

area samples and the low expectation from early work, WC_{1-x} has not attracted much attention as a catalyst. According to a recent theoretical analysis [22], however, the density of states (DOS) near the Fermi levels (E_F) of WC_{1-x} is about twice as large as that of W_2C and 6 times larger than that of WC. This provides a strong indication that WC_{1-x} may be the most active catalyst among the three tungsten carbide phases. Although conventional methods of preparation cannot produce WC_{1-x}, it is possible to synthesize nanoparticles of WC_{1-x} by a sonochemical reaction of $W(CO)_6$ [23,24].

In this study, composites of WC_{1-x} and Pt nanoparticles are synthesized on multiwalled carbon nanotube (MWNT) supports and their electrochemical properties are investigated. It is found that WC_{1-x} enhances the electrochemical activity of Pt nanoparticles for the HOR through H^+-spill-over.

2. Experimental

Platinum nanoparticles supported on MWNTs were synthesized by a chemical reduction method [25]. $H_2PtCl_6{\cdot}xH_2O$ (0.1792 g) and $Na_3C_6H_5O_7{\cdot}2H_2O$ (0.2571 g) were dissolved in 250 ml of de-ionized water. 0.2 g of MWNT (Iljin Nanotech Co.) was sonically dispersed in 200 ml of de-ionized water for 1 h. The two solutions were mixed and a cold $NaBH_4$ solution was added dropwise to the mixture. The solution was stirred vigorously at room temperature for 9 h. After completion of the reaction, the Pt-loaded MWNT product (Pt/MWNT) was filtered, washed thoroughly with ethanol, and placed in a vacuum desiccator for drying over a period of 10 h. WC_{1-x} nanoparticles were formed on the MWNT or Pt/MWNT supports by a sonochemical method [23,24,26]. $W(CO)_6$ (Aldrich, sublimed, 99.9+%) and a support were dispersed in 30 ml of hexadecane (Alfa Aesar, 99%) and irradiated by high-intensity ultrasound (Sonic and Materials, model VC-500, amplitude 25%, 13 mm solid probe, 20 kHz) at 85–95 °C under an argon flow for 3 h. The resultant powder was filtered, washed with pentane under a vacuum, and heat-treated at 450 °C in H_2 (50 cc min^{-1}) for 12 h. The product on MWNT is denoted as WC_{1-x}/MWNT and the composite product on Pt/MWNT as WC_{1-x}/Pt/MWNT. A second type of composite (Pt–WC_{1-x}/MWNT) was prepared by mixing Pt/MWNT and WC_{1-x}/MWNT.

The crystallinity, structure and size of the electrocatalysts were characterized with an X-ray diffractometer (XRD, DC/Max 2000, Rigaku, Cu Kα (λ = 1.54056 Å)) and a JSM-3011 high-resolution transmission electron microscope (TEM) operating at 300 kV. The elemental compositions were obtained by an energy dispersive X-ray (EDX) analyzer attached to a JEOL JSM6700F field emission scanning electron microscopy with a 5000× magnification. For each sample, the compositions of five different areas were measured and averaged.

The electrocatalytic activity was studied with a standard three-electrode electrochemical cell equipped with a rotating disc electrode (RDE, AUTOLAB), a Ag|AgCl reference electrode, and a Pt mesh counter-electrode. 10 mg of an electrocatalyst was dispersed in 5 g of de-ionized water by sonication. 5 μl of the suspension was dropped onto the working electrode (glassy carbon, d = 3 mm) and dried in air. 5 μl of a 0.05 wt.% Nafion solution was applied to cover the working electrode for mechanical protection during the rotation of the RDE. The working electrode was cleaned electrochemically before the measurements. Cyclic voltammograms (CV) were measured in a 0.5 M $HClO_4$ aqueous solution at a scan rate of 50 mV s^{-1}. The electrocatalytic activity for the HOR was evaluated by linear sweep voltammetry in 30 min-H_2 saturated electrolyte (0.5 M $HClO_4$) at a scan rate of 5 mV s^{-1} and at various rotation rates from 400 to 3600 rpm. The reported potentials are referenced to the reversible hydrogen electrode (RHE).

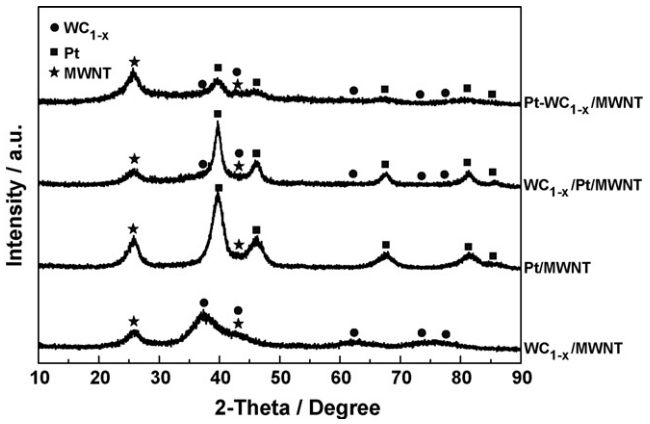

Fig. 1. XRD patterns of Pt–WC_{1-x}/MWNT, WC_{1-x}/Pt/MWNT, Pt/MWNT, and WC_{1-x}/Pt/MWNT.

3. Results and discussion

In this study, electrocatalysts composed of Pt and WC_{1-x} nanoparticles on MWNTs are prepared to examine the possibility of a co-catalyst effect of tungsten carbide nanoparticles with Pt. The sonochemical method was chosen for the synthesis of tungsten carbide nanoparticles because it has the advantage of forming very small (2–3 nm in size) nanoparticles. It should be noted that the sonochemical reaction produces WC_{1-x} nanoparticles with a fcc (face-centered cubic) structure which is different from the W_2C or the WC phases reported by other workers [8–10,14–17]. According to the phase diagram [19], WC_{1-x} is a high-temperature phase, stable above 2785 °C. It has been synthesized only as a bulk sample except for nanoparticles synthesized by sonochemistry [23,24].

The composition of the WC_{1-x}/Pt/MWNT composite was 27 wt.% WC_{1-x} and 11 wt.% Pt, as determined by EDX. A reference sample composed of 20 wt.% Pt without WC_{1-x} (Pt/MWNT) and another composed of 43 wt.% WC_{1-x} without Pt (WC_{1-x}/MWNT) were also prepared. A second form of composite (Pt–WC_{1-x}/MWNT) was obtained by physically mixing Pt/MWNT and WC_{1-x}/MWNT in proportions that made the ratio between Pt and WC_{1-x} the same as in WC_{1-x}/Pt/MWNT.

The XRD patterns of the above materials are presented in Fig. 1. The pattern for Pt/MWNT shows peaks arising from the Pt nanoparticles (fcc structure; JCPDS card no. 04-0802) and MWNT, whereas the pattern for WC_{1-x}/MWNT can be assigned to WC_{1-x} (fcc structure; JCPDS card no. 20-1316) with no indication of WC or W_2C and peaks for Pt. The particle sizes, estimated by using the Scherrer equation, are 4.1 nm for Pt in Pt/MWNT and 2.5 nm for WC_{1-x} in WC_{1-x}/MWNT. The peaks of Pt have become sharper than those in Pt/MWNT, probably because the Pt particles have grown during the sonochemical reaction and heat-treatment to form WC_{1-x} nanoparticles. The diffraction peaks of Pt and WC_{1-x} in WC_{1-x}/Pt/MWNT are broad and overlap with each other, so that estimation of the particle sizes is difficult. Nevertheless, the lowest limit of the Pt size in WC_{1-x}/Pt/MWNT, is calculated to be 7.5 nm. Therefore, the specific surface area of Pt in WC_{1-x}/Pt/MWNT is about 1.8 (= 7.5/4.1) times smaller than the others.

The TEM data for the above samples are given in Fig. 2. Pt/MWNT is composed of well-dispersed Pt nanoparticles of about 5 nm in size, which is in agreement with the XRD data (Fig. 2(A)). The TEM image of WC_{1-x}/MWNT in Fig. 2(B) shows that WC_{1-x} is formed like stains on the MWNT surfaces. This is probably because the very small WC_{1-x} nanoparticles aggregate to form islands of thin layers on the MWNT surfaces. The morphology of the composite WC_{1-x}/Pt/MWNT (Fig. 2(C) and (D)) is similar to that of WC_{1-x}/MWNT. The EDX spectrum in the inset of Fig. 2(D), which

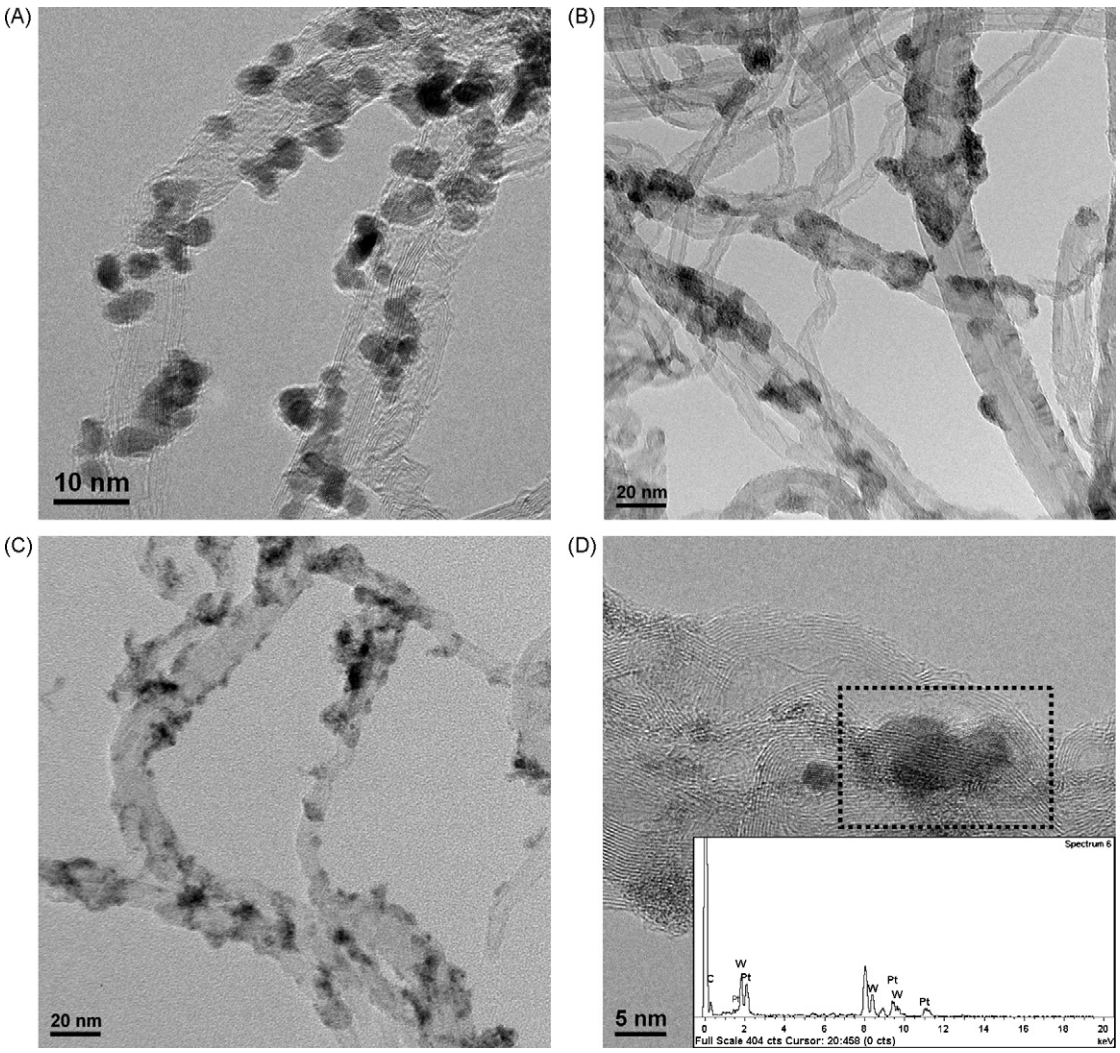

Fig. 2. TEM images of (A) Pt/MWNT, (B) WC_{1-x}/MWNT, (C) WC_{1-x}/Pt/MWNT, and (D) HRTEM image of WC_{1-x}/Pt/MWNT. Inset in (D) is EDS spectrum of marked area.

is taken for the marked area in the same figure, shows the peaks of W and Pt, and thereby indicates that each of the dark spots in Fig. 2(C) and (D) is constituted of Pt and WC_{1-x}. This suggests that the Pt nanoparticles in Pt/MWNT function as nucleation sites for WC_{1-x}, which is very likely according to the following mechanism of sonochemistry [27–29]. During the sonication process, the reagent $W(CO)_6$ is volatilized into bubbles. When the bubbles collapse, part of the mechanical impact is transferred to the $W(CO)_6$ molecules and induces their decomposition into solid precursors, which will transform into WC_{1-x} during the subsequent heat-treatment. The conversion of mechanical energy into chemical energy is known to be very inefficient. It appears, however, that solid supports can facilitate the conversion to some extent by absorbing the mechanical energy of the imploding bubbles. In certain cases, the effect of a solid support could be as dramatic as found in our previous work, in which WC_{1-x} was formed only when solid support was present [23]. The effect of the solid support will increase as the mass of the support increases. Therefore, Pt nanoparticles are much more efficient nucleation sites than uncovered MWNT surface for the deposition of WC_{1-x} precursors. Based on this, it is concluded that most of the WC_{1-x} nanoparticles in WC_{1-x}/Pt/MWNT are in close contact with Pt nanoparticles. The aggregation of the WC_{1-x} nanoparticles in WC_{1-x}/MWNT (Fig. 2(B)) can also be explained in terms of the already formed precursor deposits functioning as nucleation sites for the forthcoming precursors.

The four materials mentioned above were mounted in a RDE apparatus for electrochemical studies. As noted above, care was taken when preparing the electrodes so that WC_{1-x}/Pt/MWNT and Pt–WC_{1-x}/MWNT had the same amounts of electrochemically active components (Pt and WC_{1-x}) (Table 1). Therefore, the difference in the electrochemical properties between WC_{1-x}/Pt/MWNT and Pt–WC_{1-x}/MWNT can be attributed to the different methods of preparation that are considered to produce different degrees of contact between WC_{1-x} and Pt nanoparticles and a slightly larger size of Pt nanoparticle in WC_{1-x}/Pt/MWNT.

The CV data for the materials are compared in Fig. 3(A). WC_{1-x}/MWNT shows a peak at 0.1 V in the positive-going sweep. Its reversible nature suggests that WC_{1-x} is active for H^+ adsorption. WC_{1-x}/MWNT does not, however, show any signal for the HOR (Fig. 4(A)). The presence of WC_{1-x} nanoparticles results in a few changes in the CV of Pt, regardless the method of preparation. The signal for PtO formation and its reduction is suppressed (WC_{1-x}/Pt/MWNT and Pt–WC_{1-x}/MWNT in Fig. 3(A)). The peak at ~0.14 V of Pt/MWNT is suppressed and a new peak at ~0.3 V emerges, and thereby indicates H^+-spill-over. Previous studies on the other tungsten carbide phases, e.g., WC and W_2C, revealed that they have the H^+-spill-over effect when in contact with Pt [9,10,14,18]. Therefore, the H^+-spill-over effect of WC_{1-x} found in this study can be understood given its similar chemical and electronic properties to WC and W_2C phases [7,22]. Fig. 3(B) compares

Table 1
Electrode materials and their elemental compositions.

Electrocatalyst	Metal content[a] (wt.%)		Elemental quantity on the electrode[b] (μg)		
	Pt	W	Pt	W	C
Pt/MWNTs	20	0	2.0	0.0	7.7
WC_{1-x}/Pt/MWNTs	11	27	1.1	2.7	5.6
Pt–WC_{1-x}/MWNTs	13	32	1.1	2.7	12.3
WC_{1-x}/MWNTs	0	43	0.0	8.5	8.5

[a] Data obtained from EDX.
[b] Area of working electrode is 0.071 cm^2.

the ECAs of the electrode materials. The values were obtained with reference to 210 μC cm^{-2} for polycrystalline Pt [30]. Note that Pt/MWNT has about twice the amount of Pt than in the other two materials. Nevertheless, Pt–WC_{1-x}/MWNT and Pt/MWNT have almost the same ECA, which can be explained in terms of H^+-spill-over even though the Pt and WC_{1-x} nanoparticles do not have good contact. WC_{1-x}/Pt/MWNT shows a greatly increased ECA, and thereby demonstrates that the H^+-spill-over effect is much enhanced by the intimate contacts between Pt and WC_{1-x} nanoparticles in this sample. It is worth noting that the Pt nanoparticles have grown in size during the sonochemical formation of WC_{1-x} nanoparticles. Therefore, the ECA may be further increased if the size of the Pt nanoparticles is not increased.

The HOR data of the electrode materials are given in Fig. 4. As seen in Fig. 4(A), the current densities are in the order of Pt–WC_{1-x}/MWNT > WC_{1-x}/Pt/MWNT > Pt/MWNT for both the kinetic-controlled and diffusion-controlled regions. By contrast, the

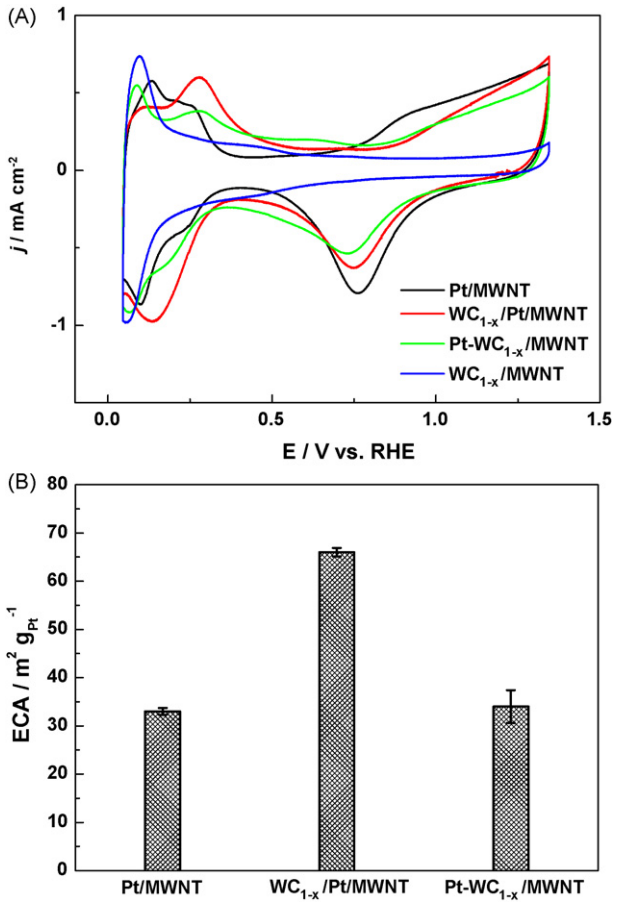

Fig. 3. (A) CVs of Pt/MWNT, WC_{1-x}/Pt/MWNT, Pt–WC_{1-x}/MWNT, and WC_{1-x}/MWNT in 0.5 M $HClO_4$ saturated with N_2 at 25 °C, scan rate: 50 mV s^{-1}. (B) ECAs of different electrocatalysts calculated from hydrogen adsorption/desorption areas in CVs.

WC_{1-x}/MWNT does not show any activity for the HOR. The results from experiments at various rotating speeds were used to derive the Koutecky–Levich plots in Fig. 4(B) using the following equations:

$$j_d = 0.62nFD_0^{2/3}\nu^{-1/6}C_0\omega^{1/2} = BC_0\omega^{1/2} \quad (1)$$

$$j^{-1} = j_k^{-1} + j_d^{-1} = j_k^{-1} + (BC_0\omega^{1/2})^{-1} \quad (2)$$

where j is the experimentally observed current density based on the geometric area of a working electrode; j_k is the kinetic current density; j_d is the diffusion-limited current density; n is the number of electrons transferred; F is the Faraday constant; D_0 is the diffusion coefficient of H_2 in $HClO_4$; ν is the kinematic viscosity of the electrolyte; C_0 is the H_2 concentration in the electrolyte; ω is rotation rate [31]. The Pt-specific mass activities (j_{mass}) of the electrodes, calculated from Koutecky–Levich plots, are compared in Fig. 4(C). The j_{mass} values of the two electrodes with WC_{1-x} nanoparticles are twice more than that of Pt/MWNT, despite the fact that the latter has twice more Pt than the former two. These observations can be explained as the consequence of an increase in the ECA by combining WC_{1-x} nanoparticles with Pt nanoparticles. Nevertheless, even though the ECA of WC_{1-x}/Pt/MWNT is almost twice that of Pt-WC_{1-x}/MWNT, their j_{mass} values are close to each other. This is probably because the surface area of the Pt nanoparticles in WC_{1-x}/Pt/MWNT is considerably reduced by the formation process of the WC_{1-x} nanoparticles. The sonochemical treatment and following heat-treatment increase the Pt particle size from 4.1 nm to a minimum 7.5 nm and part of the Pt surface is covered by WC_{1-x} nanoparticles. Therefore, if the Pt particle size can be maintained while forming WC_{1-x} nanoparticles, it seems that the HOR activity of WC_{1-x}/Pt/MWNT electrode can be further increased. More desirably, if WC_{1-x} nanoparticles are formed first and then Pt nanoparticles are grown on top, the HOR characteristics of the WC_{1-x}–Pt composite electrode may be maximized. Unfortunately, it has been found that the WC_{1-x} nanoparticles are not very stable under the formation conditions for Pt nanoparticles [32]. Furthermore, reversing the order of formation of the nanoparticles loses the advantage of the sonochemical method in which WC_{1-x} nanoparticles are preferentially formed on Pt nanoparticles to provide an intimate level of contact.

Our data clearly demonstrate that WC_{1-x} nanoparticles promote the electrochemical performance of Pt. These results are in agreement with the theoretical prediction based on the fact that WC_{1-x} has a high DOS near E_F [22].

Finally, it is noted that Santos et al. [8] have studied a similar system to that presented here. They first synthesized W_2C sonochemically on a carbon support, and then formed Pt nanoparticles. The CV of their Pt–W_2C/C was very similar to that of Pt/C, and although the presence of W_2C increased the kinetics, the difference was very small, contrary to our results. This difference in results may have arisen because the amount of tungsten carbide in our materials is much larger than that in the other study. Nevertheless, based on the theoretical prediction that W_2C is more W-like than WC_{1-x} [22], it seems that the different electronic structures between WC_{1-x} and W_2C are a more decisive cause.

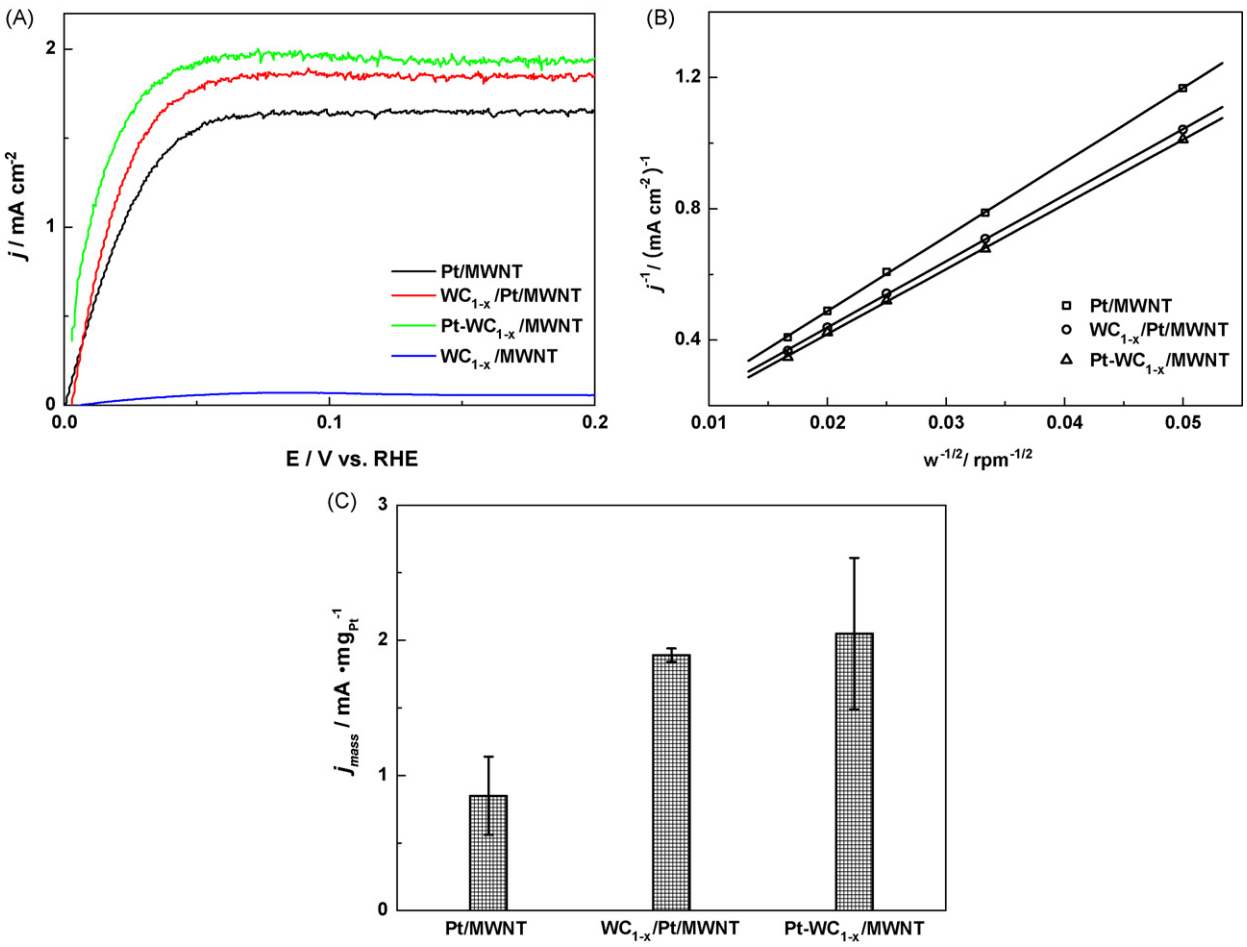

Fig. 4. (A) Linear sweep voltammograms of Pt/MWNT, WC_{1-x}/Pt/MWNT, Pt–WC_{1-x}/MWNT, and WC_{1-x}/MWNT in 0.5 M $HClO_4$ saturated with H_2 at 25 °C with 1600 rpm, scan rate: 5 mV s^{-1}. (B) Koutecky–Levich plot of HOR at 0.2 V by electrocatalysts. (C) Pt-specific mass activities of different electrocatalysts.

4. Conclusion

A study has been made of the synergistic effects between Pt and WC_{1-x} nanoparticles with respect to the electrochemical hydrogen oxidation reaction. Sonochemistry is employed to form the WC_{1-x} nanoparticles. Cyclic voltammograms show the H^+-spill-over effect from Pt to WC_{1-x}. The electrochemically active surface area can be significantly increased by simply mixing Pt and WC_{1-x} nanoparticles. The composite material prepared by the sonochemical synthesis of WC_{1-x} on Pt-loaded MWNT has an even larger electrochemically active surface area because the WC_{1-x} and Pt nanoparticles are in good contact with each other. The Pt-specific mass activity of the hydrogen oxidation reaction is also enhanced by the presence of WC_{1-x} nanoparticles. The sonochemical technique has the advantage of forming WC_{1-x} nanoparticles, which are predicted to be the most active among the tungsten carbide phases. Moreover, these nanoparticles are formed in close contact with Pt nanoparticles, by which the H^+-spill-over effect can be maximized. On the other hand, partial loss of the Pt surface area by this method has to be overcome for better performance. Future research directed towards the formation of tungsten carbide that interfaces with small Pt nanoparticles and stabilizes the WC_{1-x} phase may further increase the electrochemical activity.

Acknowledgements

This work was supported by the Korea Research Foundation Grant funded by the Korean Government (MOEHRD) (KRF-2005-005-J11903). The authors are grateful to the Samsung Advanced Institute of Technology for the financial support. The authors thank CCRF and KBSI for the TEM analysis, and Prof. S. Park for helpful discussion.

References

[1] B.C.H. Steele, A. Heinzel, Nature 414 (2001) 345–352.
[2] R.B. Levy, M. Boudart, Science 181 (1973) 547–549.
[3] L.H. Bennett, J.R. Cuthill, A.J. Mcalister, N.E. Erickson, R.E. Watson, Science 184 (1974) 563–565.
[4] R.J. Colton, J.J. Huang, J.W. Rabalais, Chem. Phys. Lett. 34 (1975) 337–339.
[5] D.V. Sokolsky, V.S. Palanker, E.N. Baybatyrov, Electrochim. Acta 20 (1975) 71–77.
[6] M. Nagai, M. Yoshida, H. Tominaga, Electrochim. Acta 52 (2007) 5430–5436.
[7] Y. Hara, N. Minami, H. Itagaki, Appl. Catal. A 323 (2007) 86–93.
[8] L.G.R.A. Santos, K.S. Freitas, E.A. Ticianelli, J. Solid State Electrochem. 11 (2007) 1541–1548.
[9] R. Ganesan, J.S. Lee, Angew. Chem., Int. Ed. 44 (2005) 6557–6560.
[10] R. Ganesan, D.J. Ham, J.S. Lee, Electrochem. Commun. 9 (2007) 2576–2579.
[11] E.C. Weigert, A.L. Stottlemyer, M.B. Zellner, J.G. Chen, J. Phys. Chem. C 111 (2007) 14617–14620.
[12] H.H. Hwu, B.D. Polizzotti, J.G. Chen, J. Phys. Chem. B 105 (2001) 10045–10053.
[13] D.R. McIntyre, G.T. Burstein, A. Vossen, J. Power Sources 107 (2002) 67–73.
[14] M.K. Jeon, H. Daimon, K.R. Lee, A. Nakahara, S.I. Woo, Electrochem. Commun. 9 (2007) 2692–2695.
[15] D.J. Ham, Y.K. Kim, S.H. Han, J.S. Lee, Catal. Today 132 (2008) 117–122.
[16] H. Meng, P.K. Shen, J. Phys. Chem. B 109 (2005) 22705–22709.
[17] M. Nie, P.K. Shen, M. Wu, Z. Wei, H. Meng, J. Power Sources 162 (2006) 173–176.
[18] M.K. Jeon, K.R. Lee, W.S. Lee, H. Daimon, A. Nakahara, S.I. Woo, J. Power Sources 185 (2008) 927–931.
[19] A.S. Kurlov, A.I. Gusev, Inorg. Mater. 42 (2006) 121–127.
[20] T. Xiao, A. Hanif, A.P.E. York, J. Sloan, M.L.H. Green, Phys. Chem. Chem. Phys. 4 (2002) 3522–3529.
[21] M.B. Zellner, J.G. Chen, Catal. Today 99 (2005) 299–307.

[22] D.V. Suetin, I.R. Shein, A.L. Ivanovskii, J. Phys. Chem. Solids 70 (2009) 64–71.
[23] H. Park, M.H. Kim, Y.K. Hwang, J.S. Chang, Y.U. Kwon, Chem. Lett. 34 (2005) 222–223.
[24] J.D. Oxley, M.M. Mdleleni, K.S. Suslick, Catal. Today 88 (2004) 139–151.
[25] J. Zeng, J.Y. Lee, W. Zhou, Appl. Catal. A 308 (2006) 99–104.
[26] T. Hyeon, M. Fang, K.S. Suslick, J. Am. Chem. Soc. 118 (1996) 5492–5493.
[27] K.S. Suslick, D.A. Hammerton, R.E. Cline Jr., J. Am. Chem. Soc. 108 (1986) 5641–5642.
[28] K.S. Suslick, S.B. Choe, A.A. Cichowlas, M.W. Grinstaff, Nature 353 (1991) 414–416.
[29] K.S. Suslick, T. Hyeon, M. Fang, Chem. Mater. 8 (1996) 2172–2179.
[30] M.J.J. Mayrhofer, D. Strmcnik, B.B. Blizanac, W. Stamenkovic, M. Arenz, N.M. Markovic, Electrochim. Acta 52 (2008) 3181–3188.
[31] A.J. Bard, L.R. Faulkner, Electrochemical Methods: Fundamentals and Applications, second ed., John Wiley & Sons, Inc., New York, 2001, p. 339–343.
[32] K.M. Andersson, L. Bergstrom, Int. J. Refract. Met. Hard Mater. 18 (2000) 121–129.